

1 Supplementary Figures

2 Ecosystem Climate Sensitivities Drive the Divergence in
3 Aerosol-Induced Carbon Uptake Across CMIP6 Models

4 Zhaoyang Zhang¹, Meng Fan^{2*}, Minghui Tao³, Yunhui Tan⁴, Quan Wang⁴

5 1. College of Geography and Environmental Sciences, Zhejiang Normal University,
6 Zhejiang Province 321000, China

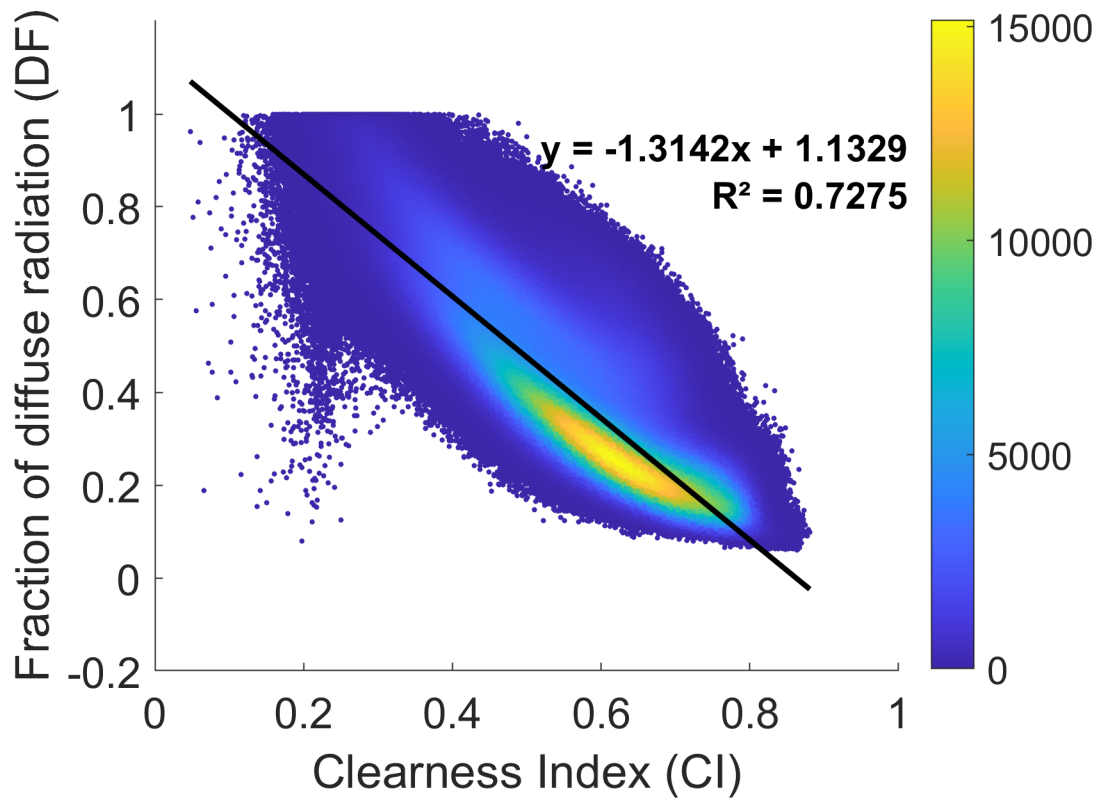
7 2. Aerospace Information Research Institute, Chinese Academy of Sciences, Beijing
8 100101, China

9 3. School of Geography and Information Engineering, China University of
10 Geosciences, Wuhan 430074, China

11 4. Faculty of Agriculture, Shizuoka University, Shizuoka 4228529, Japan

12 *Corresponding author: Meng Fan (fanmeng@aircas.ac.cn)

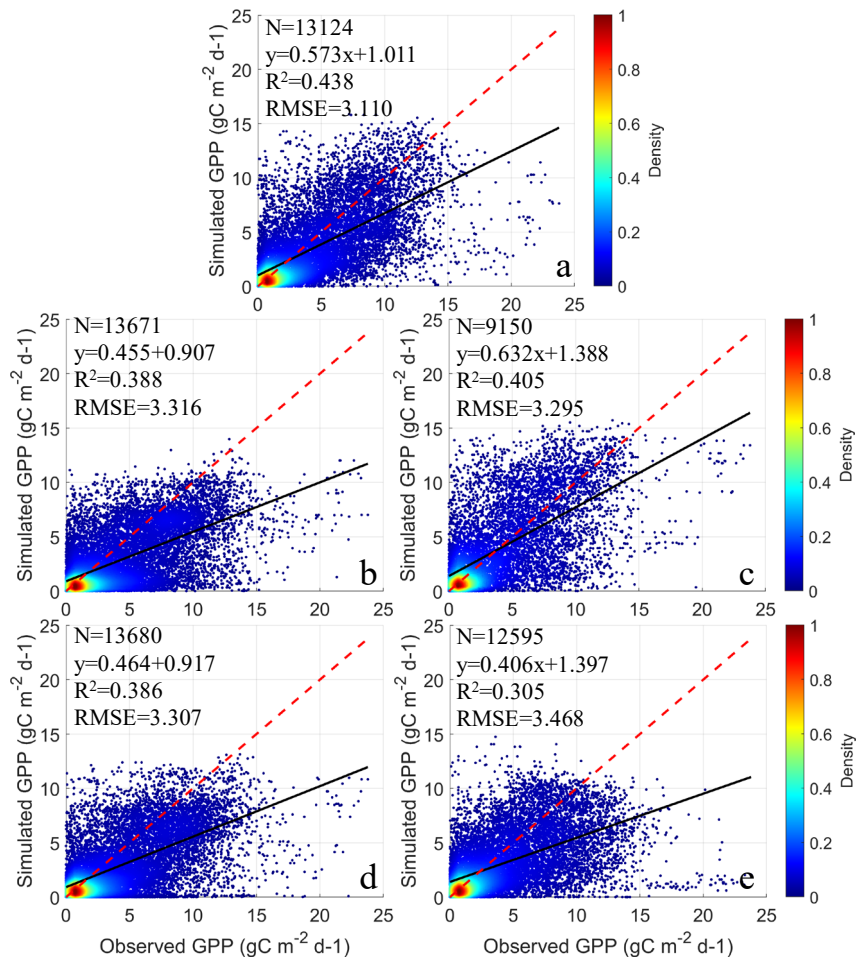
13



14

15 Figure S1. The scatter plots of fraction of diffuse radiation (DF) against the clearness index (CI)

16 from NorESM2-LM and UKESM1-0-LL.

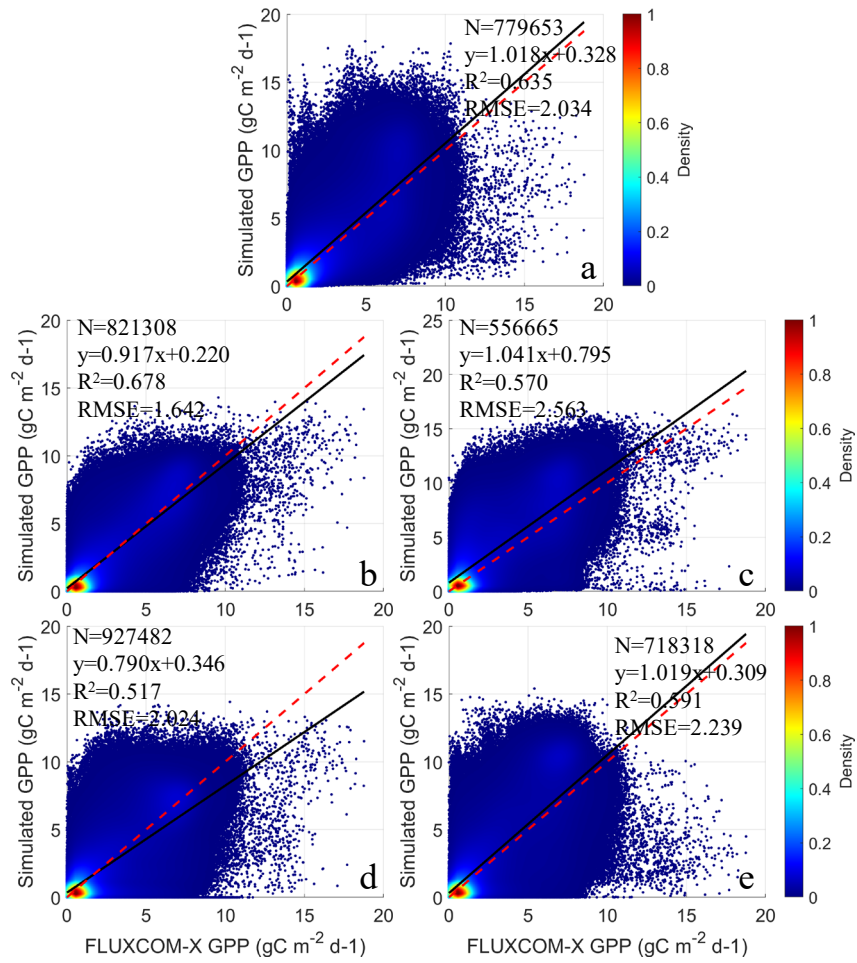


17

18 Figure S2. The scatter plots of simulated monthly GPP from CMIP6 models (a. BCC-ESM1, b. IPSL-

19 CM6A-LR, c. MPI-ESM-1-2-HAM, d. NorESM2-LM, e. UKESM1-0-LL) against observed GPP from

20 FLUXNET sites.

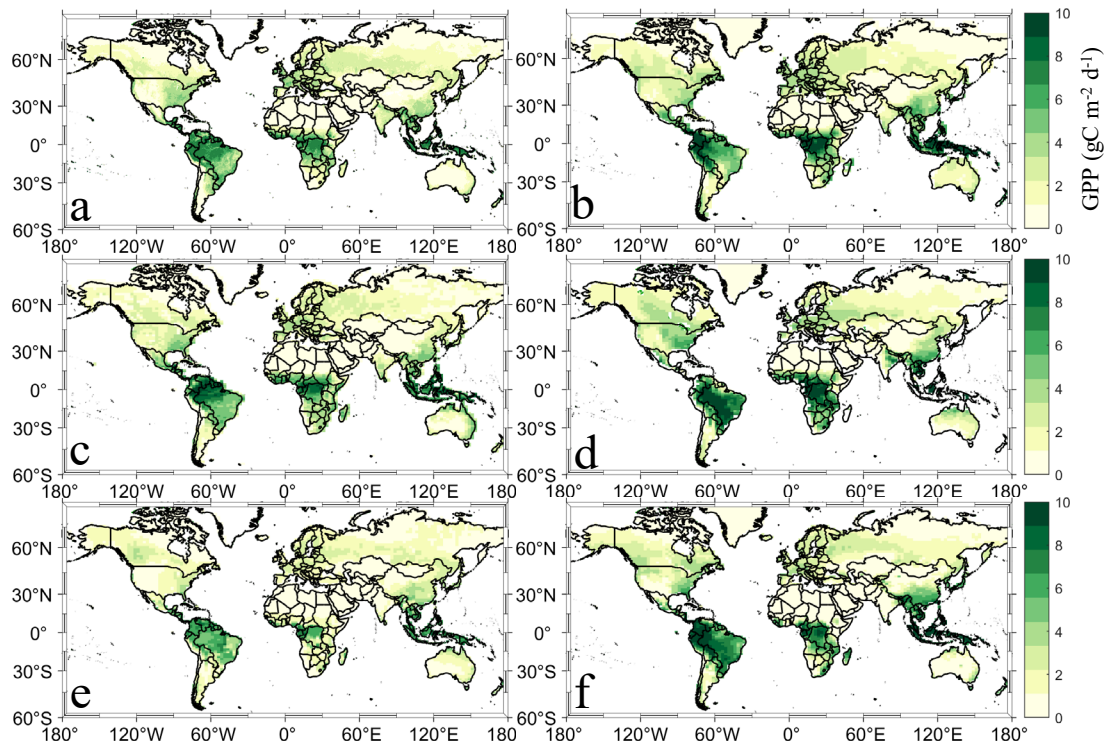


21

22 Figure S3. The scatter plots of simulated monthly GPP from CMIP6 models (a. BCC-ESM1, b. IPSL-

23 CM6A-LR, c. MPI-ESM1-2-HAM, d. NorESM2-LM, e. UKESM1-0-LL) against GPP from

24 FLUXCOM-X.



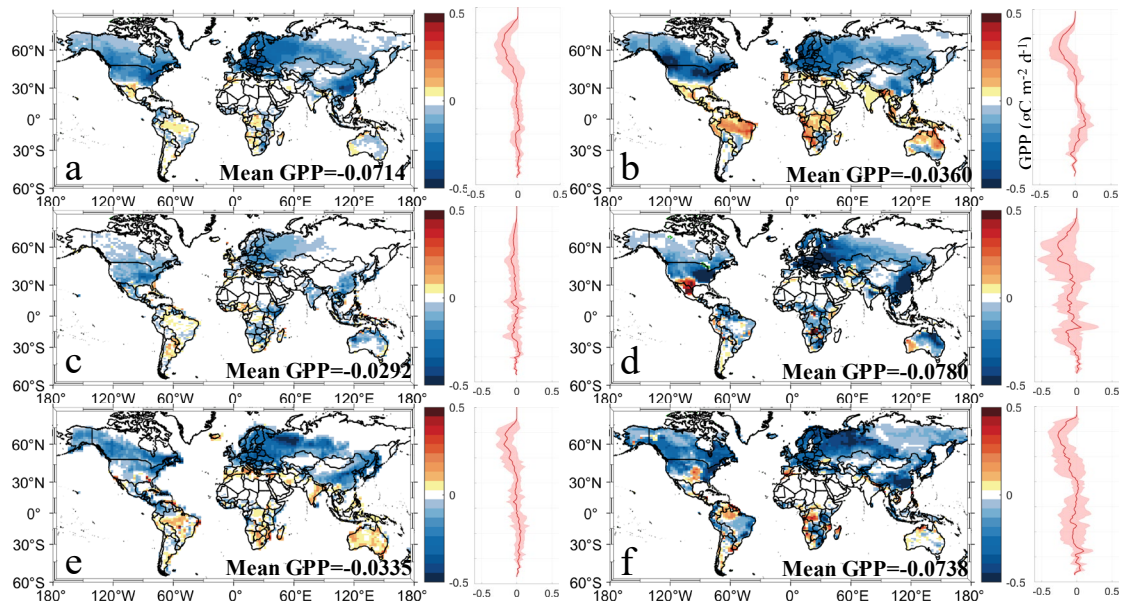
25

26 Figure S4. The spatial distribution of observed and simulated GPP from 2001 to 2014 (a. FLUXCOM-

27 X, b. BCC-ESM1, c. IPSL-CM6A-LR, d. MPI-ESM-1-2-HAM, e. NorESM2-LM, f. UKESM1-0-LL).

28

29



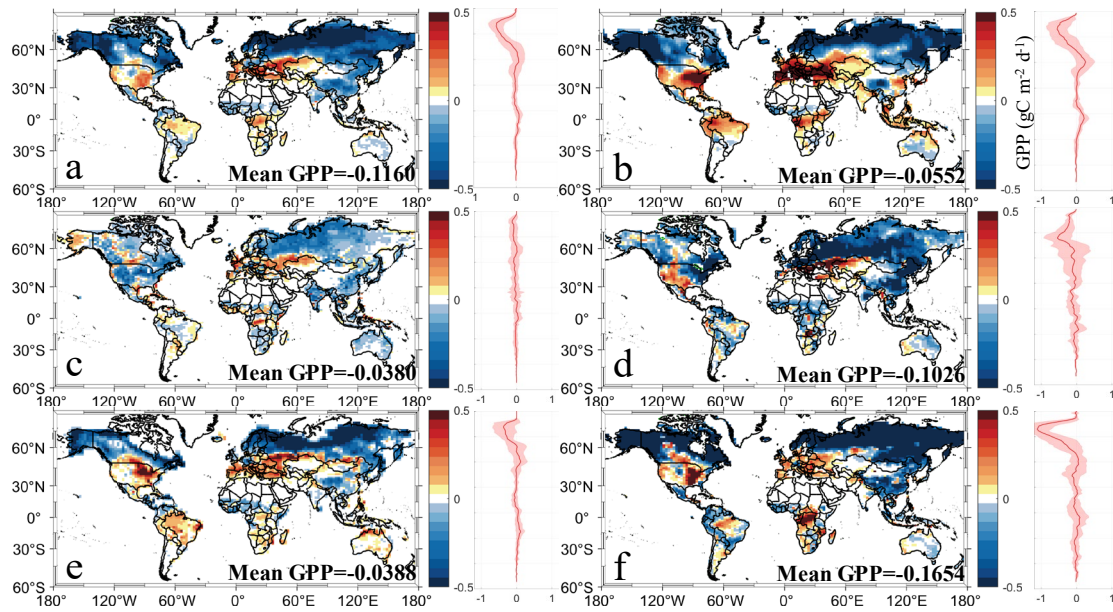
31

32 Figure S5. The spatial pattern of changes in ecosystem GPP induced by aerosols from CMIP6 models (a.

33 multi-model mean, b. BCC-ESM1, c. IPSL-CM6A-LR, d. MPI-ESM-1-2-HAM, e. NorESM2-LM, f.

34 UKESM1-0-LL) from March to May.

35



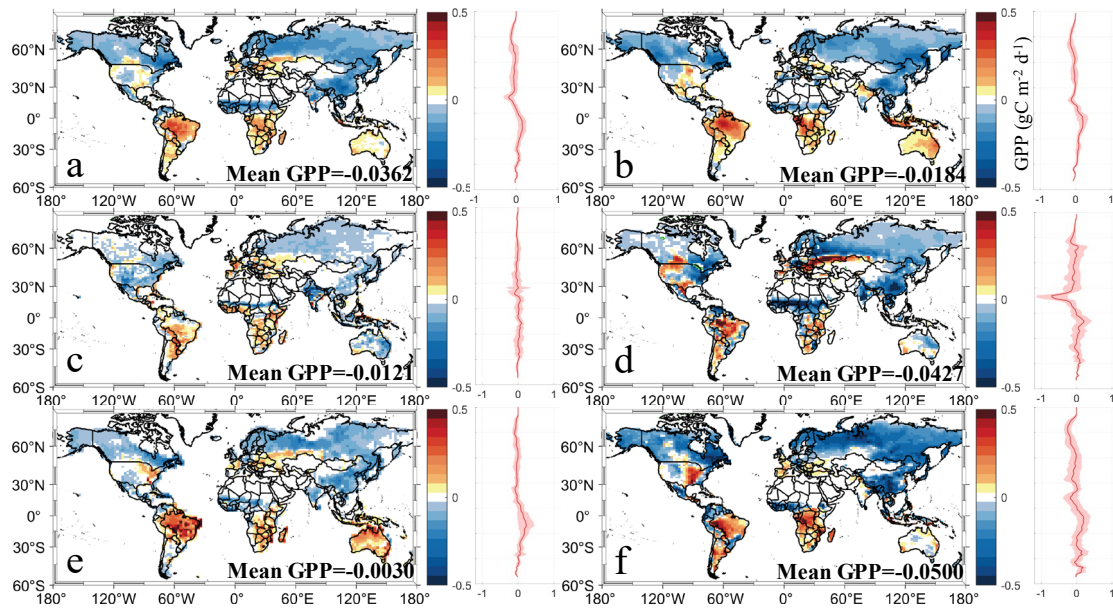
37

38 Figure S6. The spatial pattern of changes in ecosystem GPP induced by aerosols from CMIP6 models (a.

39 multi-model mean, b. BCC-ESM1, c. IPSL-CM6A-LR, d. MPI-ESM-1-2-HAM, e. NorESM2-LM, f.

40 UKESM1-0-LL) from June to August.

41



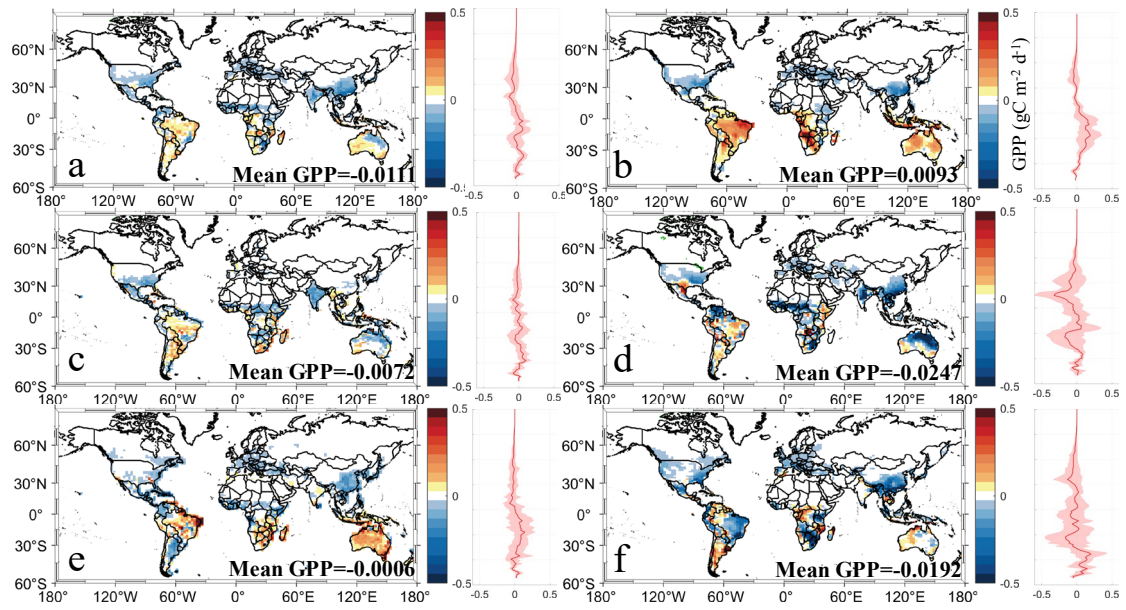
43

44 Figure S7. The spatial pattern of changes in ecosystem GPP induced by aerosols from CMIP6 models (a.

45 multi-model mean, b. BCC-ESM1, c. IPSL-CM6A-LR, d. MPI-ESM-1-2-HAM, e. NorESM2-LM, f.

46 UKESM1-0-LL) from September to November.

47



49

50 Figure S8. The spatial pattern of changes in ecosystem GPP induced by aerosols from CMIP6 models (a.

51 multi-model mean, b. BCC-ESM1, c. IPSL-CM6A-LR, d. MPI-ESM-1-2-HAM, e. NorESM2-LM, f.

52 UKESM1-0-LL) from December to February.

53